Sina Gilassi and Nejat Rahmanian*

CFD Modelling of a Hollow Fibre Membrane for CO_2 Removal by Aqueous Amine Solutions of MEA, DEA and MDEA

Abstract: A mass transfer model was developed to capture CO_2 from a gas mixture in hollow fibre membrane contactors under laminar flow conditions. The axial and radial diffusions through membrane and convection in tube and shell sides with chemical reaction were investigated. COMSOL software was used to numerically solve a system of non-linear equations with boundary conditions by use of the finite element method. Three different amine solutions of monoethanolamine (MEA), diethanolamine (DEA) and *n*-methyldiethanolamine (MDEA) were chosen as absorbent in lumen to consider the mass transfer rate of CO_2 and its removal efficiency. The modelling results were compared with experimental data available in the literature and a good agreement was observed. The CFD results revealed that MEA had the best performance for CO_2 removal as compared to DEA and MDEA under various operating conditions due to the different CO_2 loading factor of absorbents. Furthermore, efficiency of CO_2 removal was highly dependent on the absorbent concentration and flow rate, increasing of the gas flow rate caused a reduction in gas residence time in the shell and consequently declined CO_2 mass transfer. The modelling results showed the effect of absorbent concentration on the CO_2 mass transfer was improved due to availability of absorbent reactants at the gas-liquid interface.

Keywords: amine solutions, CFD modelling, CO_2 separation, hollow fibre membrane

1 Introduction

One of the most current controversial topics is the effect of greenhouse gases on the environment which causes climate change and global warming. The CO_2 emission

*Corresponding author: Nejat Rahmanian, School of Engineering and Informatics, University of Bradford, Bradford, BD7 1DP, UK, E-mail: n.rahmanian@bradford.ac.uk, rahmaniyan@yahoo.com
Sina Gilassi, Department of Chemical Engineering, Universiti Teknologi PETRONAS, Bandar Seri Iskandar, 31750, Malaysia, E-mail: sina.gilassi@gmail.com

from the combustion of fossil fuels is regarded as the main contributor to the enhancement of the greenhouse effect (Halmann and Steinberg 1998). Nowadays, scientists and researchers are highly focusing on devising and improving efficient methods for mitigating CO_2 generated by industry and power plants (Casper 2010). As CO_2 constitutes a main part of flue gas and 80% of greenhouse gases, its removal by use of absorption, adsorption and membrane methods can considerably reduce and control the risk of emission problems.

The conventional separation methods for CO_2 capture based on amine absorbents are still in use, although the regeneration process is highly energy intensive and causes operational problems such as flooding and foaming (Moulijn, Makkee, and Van Diepen 2013). The commonly used absorbents are aqueous solutions of alkanolamine such as MEA, DEA and MDEA which are still used in packed columns for CO_2 removal (Veawab, Aroonwilas, and Tontiwachwuthikul 2002). The performance of these solutions was experimentally evaluated in an absorber column and revealed that MEA had the best CO_2 removal efficiency amongst DEA and MDEA solutions (Aroonwilas and Veawab 2004). By the advent of industrial membrane technology in 1980 (Baker 2012), scientists and engineers gave their attention to utilize different types of polymeric membranes in spiral-wound and hollow fibre modules. Cynara (USA) and Separex (France) were two major companies which fabricated the system for separation of CO_2 from natural gas (Baker 2012). The gas-liquid hollow fibre membrane contactor is a substantial candidate to be replaced with conventional systems in which a similar mechanism of mass transfer exists between two phases and also the rate of CO_2 absorption significantly undergoes the use of various absorbents (Li and Chen 2005). Due to the hydrophobic properties of polymeric membranes in gas separation, a solid barrier is made to impede the penetration of liquid phase into the gas phase. Instead, the gas phase completely fills the membrane pore channels and forms a gas-liquid interface. Therefore, gas diffusion occurs on account of the difference in concentration of the absorbent type more

than the pressure gradient (Mansourizadeh and Ismail 2007). In terms of membrane material selection, the hollow fiber modules are mainly dependent on the CO_2 reactivity of absorbent rather than the flat sheet modules which need a treatment method in order to alter the morphology of the polymeric membrane and enhance the separation efficiency. In this way, the measurement of permeability and selectivity of a membrane can partially simplify selection of an appropriate polymeric for a gas separation system (Gilassi and Rahmanian).

Mass transfer in hollow fibre membranes is highly dependent on the overall mass transfer which includes three individual mass transfer coefficients relating to the liquid phase, membrane, and gas phase boundary layer (Zhang and Wang 2013). The effect of partial or wetted pores on membrane mass transfer coefficient is to cause an increment because of the stagnant liquid phase in pore channels (Rangwala 1996). Mansourizadeh and Ismail (2007) studied the effect of liquid temperature and pressure on the absorption/stripping of CO_2/N_2 gas mixture by developing hydrophobic polyvinylidenefluoride (PVDF) hollow fibre membranes. Yang et al. (2012) investigated the efficiency of CO_2 removal by polypropylene (PP) hollow fibre membranes with MEA as the absorbent for removal of SO_2 content in the flue gas of power plants. They showed a good affinity between amine absorbent and sulphuric gas to remove both CO_2 and SO_2 spontaneously. Similarly, Hedayat et al. (2011) conducted removal of CO_2 and H_2S from a gas mixture similar to natural gas in PVDF and polysulfone (PSF) hollow fibre membranes simultaneously. Simulation of the CO_2 removal system is a valid method to optimize the separation by the change in operating variables such as gas and liquid velocity, membrane pressure drop and temperature for one or multi-stage separation systems. Diverse models relating to transport equations with specific model assumptions have been suggested to predict the concentration of CO_2 absorption in HFMCs using different absorbents. Zhang et al. (2006) presented a model to indicate the effect of increase in liquid flow rate on the CO_2 flux with distilled water and aqueous DEA as solvents whilst axial diffusion was neglected. They concluded that the physical reaction of CO_2 with distilled water had been less effective than the chemical reaction of CO_2 with MEA. The model by Razavi et al. (2013) showed the influence of absorbent flow rate on the efficiency of CO_2 removal based on the assumption that the velocity at the surface of the membrane was non-slip. Gilassi and Rahmanian (2014) developed a mathematical

model to predict the CO_2 concentration in a flat sheet module for CO_2/CH_4 separation and also investigated the effect of slip boundary condition at the membrane interface. The modelling result revealed that the slip condition was highly dependent on the membrane permeability and an empirical factor which caused the fluid reflection at the gas-membrane interface. The results revealed that the mass transfer model had been more accurate than the conventional model without chemical reaction. Saidi et al. (2014) developed a model to investigate the effect of DEA, MDEA and the blend of these solutions on the CO_2 capture. Their results showed that DEA solution was the best performance for CO_2 removal amongst the other solutions. In terms of model development, a numerical comparison between one and two dimensional models for CO_2 capture with MEA solution using a hollow fiber membrane was also presented by Albarracin Zaidiza et al. (2014) to examine the accuracy of developed models. Use of various absorbents has different influences on the CO_2 removal efficiency and absorbent selection is likely regarded as important criteria to optimize a separation process (Kothandaraman et al. 2009).

In this study, a two-dimensional model of mass transfer is presented to highlight the effect of absorbent type and flow rate on CO_2 concentration in a hollow fibre membrane contactor. COMSOL software was used to solve continuity and momentum equations regarding the boundary conditions at the interface of three phases. The presented model simulates the radial and axial diffusions through the membrane and convection inside shell and tube of module. This study also considers the effect of chemical reaction on the tube side between CO_2 and amine solutions of MEA, DEA and MDEA and therefore the modelling result can be confidently used to simplify the selection of efficient absorbent amongst the amine solutions. Figure 1 shows a schematic plan of a hollow fibre membrane contactor. In order to validate the model, the modelling result is compared with experimental data obtained from the literature (Yan et al. 2007).
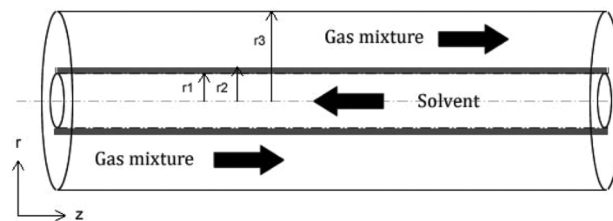

Figure 1: Schematic plan of a hollow fibre mebrane contactor.

2 Model development

A two-dimensional mass transfer model is proposed for CO_2 capture from a gas mixture of CO_2/N_2 in a hollow fibre membrane contactor. The separation is followed by a chemical reaction between the gas and liquid phases. The model is based on "non-wetting mode" so that the pore channel of the membrane is filled by the gas phase. The gas phase flows inside the shell whereas the liquid phase flows inside the tube in counter-current mode. Table 1 shows the HFMC details (Faiz and Al-Marzouqi 2009), and the model pursues the assumption as follows:

– Gas and liquid flows are in steady-state and isothermal conditions.
– Gas flow conforms to Happel's free surface model (Happel 1959) and ideal gas law.
– Equilibrium between gas-liquid phases is determined by Henry's law.
– Non-slip conditions at the membrane surface and fully developed velocity profile were seen.

Table 1: Dimension of hollow fibre membrane contactor (Faiz and Al-Marzouqi 2009).

Parameter	Values
Inner radius of tube (mm)	0.22
Outer radius of tube (mm)	0.30
Inner radius of shell (mm)	0.529
Membrane length (cm)	22
Number of fibres (–)	3600
Porosity (%)	40
Tortuosity (–)	2

2.1 Shell equations

Generally, the Navier-Stokes equations determine the velocity in the shell side for incompressible fluid and can be written as follows:

$$\frac{\partial u}{\partial t} + (u.\nabla)u = -\nabla p + v\Delta u \qquad (1)$$

$$\nabla.u = 0 \qquad (2)$$

where u (m/s) is velocity vector in the r and z directions, p (Pa) and v (cP) are pressure and viscosity, respectively. The effective radius is specified according to Happel's model (1959) and expressed as follows:

$$r_3 = \left(\frac{1}{1-\phi}\right)^{1/2} r_2 \qquad (3)$$

$$1 - \phi = \frac{nr_2^2}{R^2} \qquad (4)$$

where u, r_3, r_2 denotes the average velocity (m/s) radius of free surface (m) and fibre outer radius (m), respectively. R is the module inner radius (m), ϕ is the volume fraction of the void, and n is the number of fibres. The continuity equation containing diffusion and convection in cylindrical co-ordinates can be expressed as follows (Bird, Stewart, and Lightfoot 2007):

$$D_{shell}\left(\frac{\partial^2 C_{CO_2}}{\partial r^2} + \frac{1}{r}\frac{\partial C_{CO_2}}{\partial r} + \frac{\partial^2 C_{CO_2}}{\partial z^2}\right) = u_z\frac{\partial C_{CO_2}}{\partial z} \qquad (5)$$

where C (mol/m^3) denotes the concentration. The diffusivity coefficient D (m^2/s) is determined using the Chapman–Enskog theory (Mills 2001). Boundary conditions are expressed as follows:

$$z = L \quad C_{shell} = C_0 \qquad (6)$$

$$r = r_3 \quad \frac{\partial C_{shell}}{\partial r} = 0 \qquad (7)$$

$$r = r_2 \quad C_{shell} = C_{membrane} \qquad (8)$$

2.2 Membrane equations

The transport equation inside the membrane, which predicts CO_2 concentration, has only a diffusion term under steady-state conditions as follows:

$$D_{membrane}\left(\frac{\partial^2 C_{CO_2}}{\partial r^2} + \frac{1}{r}\frac{\partial C_{CO_2}}{\partial r} + \frac{\partial^2 C_{CO_2}}{\partial z^2}\right) = 0 \qquad (9)$$

Diffusivity coefficient in membrane, $D_{membrane}$ (m^2/s), can be calculated by eq. (10) (Al-Marzouqi et al. 2008).

$$D_{membrane} = D_{shell}\frac{\varepsilon}{\tau} \qquad (10)$$

where ε and τ are porosity and tortuosity, respectively. Boundary conditions are defined as follows:

$$r = r_2 \quad C_{membrane} = C_{shell} \qquad (11)$$

$$r = r_1 \quad C_{membrane} = C_{tube}/H \qquad (12)$$

where H is a dimensionless parameter, i.e. Henry's coefficient.

2.3 Tube equations

The continuity equation with a chemical reaction term is given by eq. (12).

$$D_{tube}\left(\frac{\partial^2 C_{CO_2}}{\partial r^2} + \frac{1}{r}\frac{\partial C_{CO_2}}{\partial r} + \frac{\partial^2 C_{CO_2}}{\partial z^2}\right) = u_z \frac{\partial C_{CO_2}}{\partial z} + R_i \qquad (13)$$

where R_i (mol/m^{3}s) is the reaction rate of CO_2 and D_{tube} (m^2/s) is diffusivity coefficient in tube which can be calculated from N_2O analogy (Versteeg and Van Swaalj 1988). The boundary conditions are expressed as follows:

$$z = 0 \quad C_{tube} = 0, C_{absorbent} = C_{absorbent-in} \qquad (14)$$

$$r = r_1 \quad C_{tube} = C_{membrane} \times H \qquad (15)$$

$$r = 0 \quad \frac{\partial C_{tube}}{\partial r} = 0 \qquad (16)$$

2.4 Reaction rate of CO_2 in amine solution

The reaction between CO_2 with amine solution involves the formation of carbamate, bicarbonate and carbamate reversion (Sakwattanapong, Aroonwilas, and Veawab 2009). The formation is expressed by the zwitterion mechanism as follows:

$$CO_2 + RR'NH \xleftrightarrow[k_{-1}]{k_2} RR'NH^+ COO^- \qquad (17)$$

$$RR'NH^+ COO^- + B \xrightarrow{k_B} BH^+ + RR'NCOO^- \qquad (18)$$

where R and R' represent C_2H_4OH, H and C_2H_4OH for primary and secondary amines, respectively. The rate of reaction of the CO_2-MEA and CO_2-DEA systems are similarly shown by eq. (18) and for CO_2-MDEA is expressed by eq. (19). The kinetic constants for MEA-H_2O solution are given in Table 2 (Paul, Ghoshal, and Mandal 2008).

$$r_{CO_2-MEA} = \frac{k_{2-MEA}[CO_2][MEA]}{1 + 1/(k_{H_2O}/(k_{-1})C_{H_2O}) + (k_{MEA})/(k_{-1})C_{MEA}}$$
$$(19)$$

$$r_{CO_2-MDEA} = k_{2-MDEA}[CO_2][MDEA] \qquad (20)$$

Table 2: Kinetic parameters at 298°K (Paul et al. 2008).

Amine aqueous solution	$k_{2-amine}$ (m^3 mol^{-1} s^1)	$k_{2-amine}k_{H_2O}/k_{-1}$ (m^6 mol^{-2} s^{-1})	$k_{2-amine}k_{amine}/k_{-1}$ (m^6 mol^{-2} s^{-1})
MEA + H_2O	6.35	9.58×10^{-6}	1.58×10^{-3}
DEA + H_2O	2.375	2.20×10^{-6}	0.43×10^{-3}
MDEA + H_2O	5.21		

3 Numerical scheme

Due to the non-linear form of equations in the suggested model, COMSOL software (ver. 4.3) was chosen to solve the equations numerically with stiff and non-stiff boundary value conditions on the basis of the finite element method. Triangular mesh type with specific size was chosen to discretize the domain and the scale factor is taken into account because of different size length and diameter of fibres. The PARDISO mode (a solver for symmetric and non-symmetric linear systems of equations) was chosen due to non-linearity of the system of equations with the minimum and maximum damping factor of 1×10^{-4} and 1×10^{-8}, respectively.

4 Model validation

The mass transfer model is validated by experimental data from the literature (Yan et al. 2007) for CO_2 removal with MEA in a hollow fibre membrane. The result of the model presented, including MEA, DEA and MDEA need to be compared with real data. As there is no available experimental data for DEA, therefore the validation is carried out only for MEA. Figures 2 and 3 show the model results which are in good agreement with the reported data. Moreover, the deviation between experimental and modelling results for the effect of liquid and gas flow rates on CO_2 mass transfer rate based on the average absolute relative error (ARRE) calculation method, are 0.75% and 8.75%, respectively.
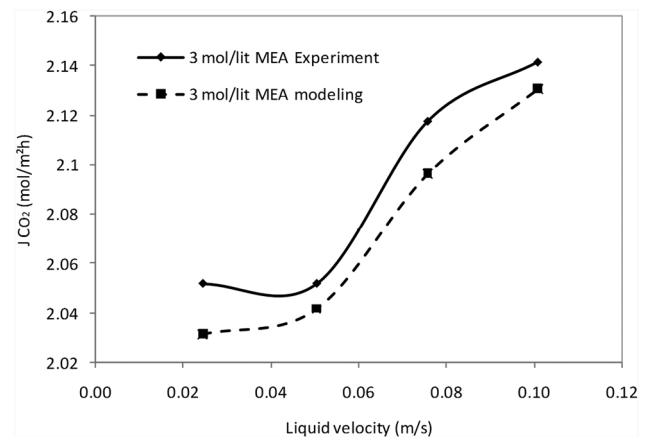
Figure 2: The effect of liquid velocity on CO_2 mass transfer rate for MEA solution.
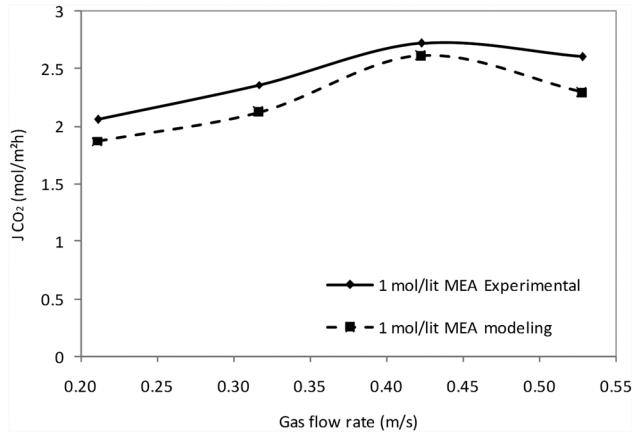
Figure 3: The effect of gas flow rate on CO_2 mass transfer rate for MEA solution.

5 Results and discussion

5.1 Velocity profile

The velocity distribution of the gas feed in the shell side is shown in Figure 4. The velocity profile is determined by solving the Navier-Stokes equations with boundary conditions at the walls and membrane surface. The pressure drop along the side of the shell was theoretically estimated by the Hagen-Poiseuille equation (Chang et al. 1998) which was considered to be approximately zero. Furthermore, the velocity near the shell side and membrane surfaces was assumed to be in an identical state which resulted in a symmetric parabolic profile, and consequently, a fully developed profile approximately at the end of the shell appears. It is worthy to mention that the velocity profile at the membrane surface varied regarding membrane structure and permeability (Nield 2009).
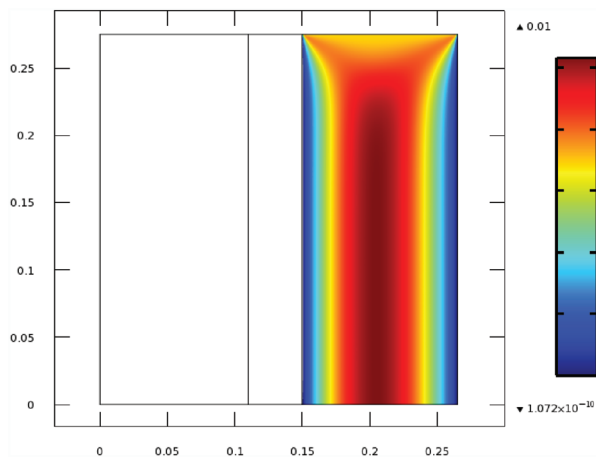

Figure 4: Velocity profile of gas feed in shell.

5.2 Effect of CO_2 concentration

The effect of CO_2 volumetric concentration in the gas feed mixture on the CO_2 mass transfer rate is shown in Figure 5. Based on the transport phenomena in the shell, there has been competition between the components of the gas mixture (N_2/CO_2) pertaining to diffusive and convective transfers. Moreover, the CO_2 concentration at the inlet is at its maximum and the concentration at the outlet is the minimum which is independent of diffusion. An increase in CO_2 concentration of gas feed causes the mass transfer rate to decrease for the three amine solutions on condition that the absorbents concentration is 3 mol/litre and gas and liquid velocity are set at minimum value. In this state, MEA shows better CO_2 removal performance than DEA. The MEA curve declines more slightly and thus displays high CO_2 loading property of that amine solution. The sharp slope of the DEA curve represents the high dependency on CO_2 concentration; the descending state can be halted by increasing the absorbent concentration in the tube side. It can be emphasised that the influence of MDEA solution is not shown in Figure 5 owing to the descriptive difference amongst the solution's curves. It is expected to compare the effect of MEA and DEA solutions separately with great accuracy. Moreover, in comparison with three types of amine solution, MEA and DEA have shown considerably better performance than MDEA.
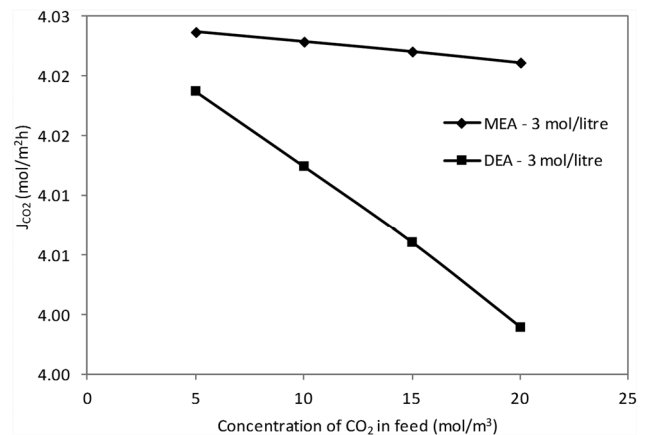

Figure 5: The effect of CO_2 concentration in feed gas on CO_2 mass transfer rate; Liquid velocity = 1.5 m/s, gas velocity = 5.5 m/s, gas pressure = 121.3 kPa and gas temperature = 298°K.

5.3 Effect of absorbent concentration

Figure 6 demonstrates the effect of absorbent concentration on the CO_2 mass transfer rate. An increase in concentration of the three amine solutions resulted in an increase
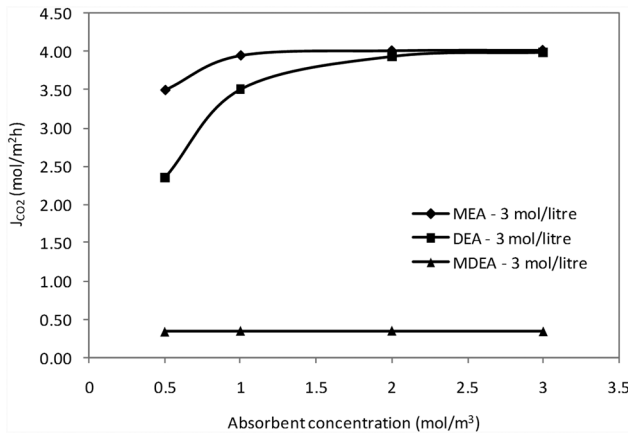
Figure 6: The effect of absorbent concentration on CO_2 mass transfer rate for different amines; Liquid velocity = 1.5 m/s, gas velocity = 5.5 m/s, CO_2 concentration = 20 % vol., gas pressure = 121.3 kPa and gas temperature = 298°K.

Figure 8: Concentration of MEA in HFMC, $C_{MEA} = 3$ mol/m^3, $C_{CO_2} = 20$ % vol., $U_g = 5.5$ m/s, $U_l = 1.5$ m/s.

of absorbent viscosity. Consequently, they can form a better reaction site at the gas-liquid interface and the CO_2 solubility significantly improves. In this case, the mass transfer rate increases swiftly for DEA solution rather than others while the CO_2 concentration of gas feed is at maximum value. In the present modelling, the concentration of CO_2 inside the shell, membrane and tube has been illustrated in Figure 7(a), 7(b), 7(c) for MEA, DEA and MDEA, respectively. CFD Simulation results illustrate the dimensionless concentration of CO_2 for all three types of amine solution in the shell in which a diverse gradient of concentration forms with respect to the absorbent capacity. It is evident that the performance of MEA is noticeably better than MDEA and DEA. MDEA cannot be a proper absorbent while the CO_2 concentration of gas feed increases. Figure 8 displays distribution of the absorbent (MEA) inside the tube. As it is expected, CO_2 component of the diffusive gas reacts with the MEA solution at the gas-liquid interface. In this way, CFD results show the depletion of the absorbent inside the tube where the MEA
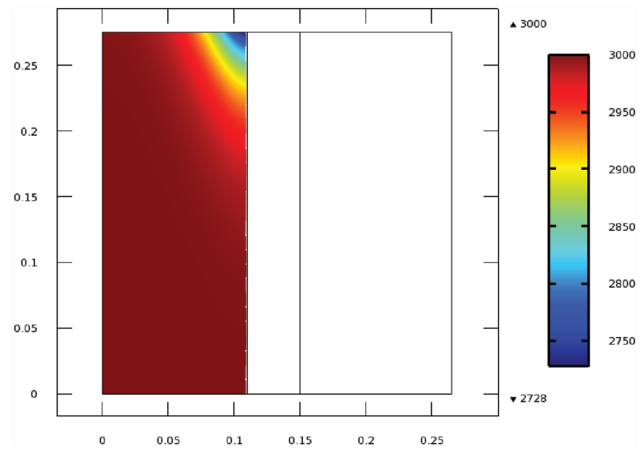
concentration profile changes at the outlet region due to the high CO_2 concentration diffused from the inlet of shell side. On the contrary, as the CO_2 concentration reduces throughout the shell, the reaction between CO_2 and absorbent at the inlet region of tube is less efficient than the outlet region of tube due to low CO_2 concentration.

5.4 Effect of gas and liquid flow rates

As the CO_2 removal efficiency is strongly dependent on the reaction between the gas and liquid phases, it is necessary to increase both gas residence time and absorbent availability at reaction active site in order to produce a more efficient reaction. It is evident that gas flow rate determines the gas residence time in the shell side and similarly through the membrane. Figure 9 shows the effect of gas velocity on CO_2 mass transfer rate. As it is seen, there are distinctive differences between the three curves of MEA, DEA and MDEA which corresponds to the performance of each absorbent to eliminate CO_2 and the
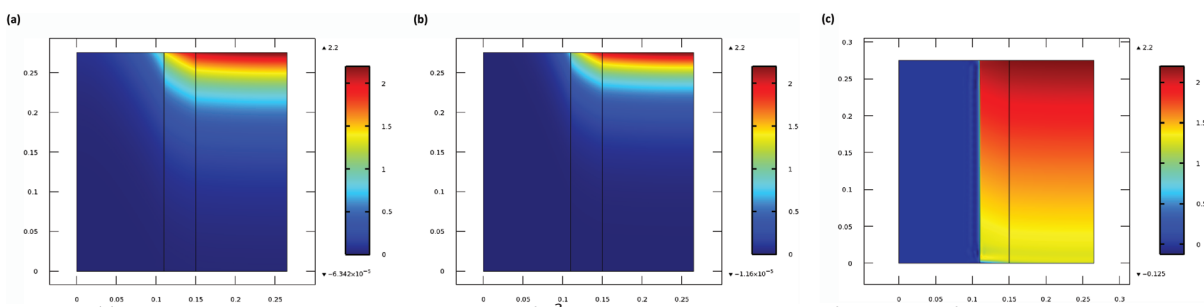

Figure 7: (a) Concentration of CO_2 in HFMC, $C_{DEA} = 3$ mol/m^3, $C_{CO_2} = 20$ % vol., $U_g = 5.5$ m/s, $U_l = 1.5$ m/s. (b) Concentration of CO_2 in HFMC, $C_{MEA} = 3$ mol/m^3, $C_{CO_2} = 20$ % vol., $U_g = 5.5$ m/s, $U_l = 1.5$ m/s. (C) Concentration of CO_2 in HFMC, $C_{MDEA} = 3$ mol/m^3, $C_{CO_2} = 20$ % vol., $U_g = 5.5$ m/s, $U_l = 1.5$ m/s.
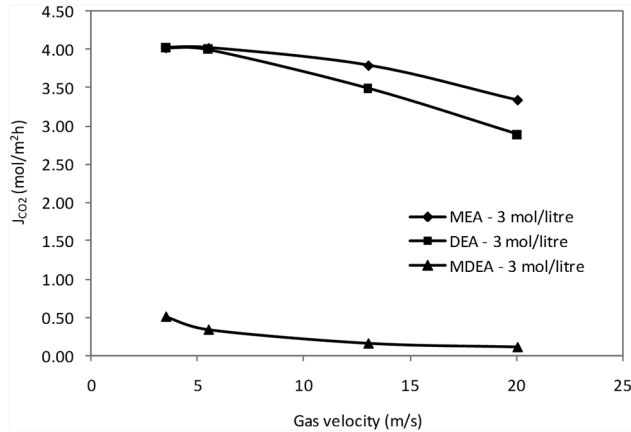
Figure 9: The effect of gas velocity on CO_2 mass transfer rate; Liquid velocity = 1.5 m/s, CO_2 concentration = 20 % vol., gas pressure = 121.3 kPa and gas temperature = 298°K.

other is an intersection point between MEA and DEA curves representing the closeness in performance of CO_2 loading property at minimum gas velocity. Moreover, an increase in gas velocity and its effect on CO_2 mass transfer rate highlights the simplicity of absorbent selection between MEA and DEA solutions. As discussed above, as the gas flow rate increases, the CO_2 flux declines steadily. In fact, the residence time of gas inside the shell is decreased by an increment of gas velocity. Then, lower amount of CO_2 is absorbed by the liquid phase even in the case that maximum concentration of the absorbent is used. With respect to liquid flow rate, Figure 10 shows the change in CO_2 flux versus to an increase in liquid velocity for MEA and DEA with equal concentration of 3 mol/litre. CO_2 mass transfer through the membrane is highly dependent on the gradient of CO_2 concentration
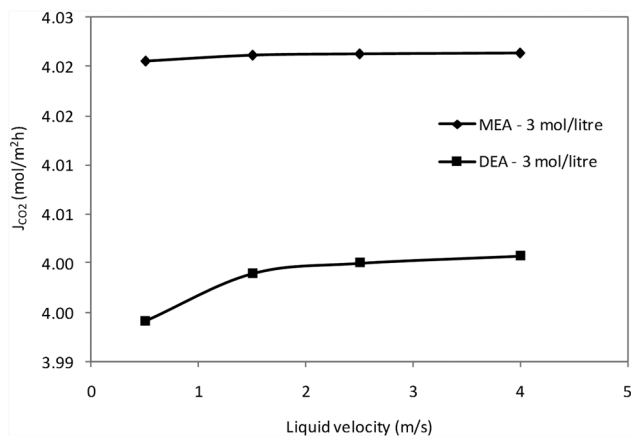

Figure 10: The effect of liquid velocity on CO_2 mass transfer rate for different amines; Gas velocity = 5.5 m/s, CO_2 concentration = 20 % vol., gas pressure = 121.3 kPa and gas temperature = 298°K.

on both sides. An increase in liquid velocity influences the CO_2 concentration at the liquid interface and produces a higher concentration gradient. It causes improvement of the mass transfer coefficient, especially for DEA solutions. The rise of CO_2 flux gradually continues, until the curve tends to level off after exceeding the effective flow rate. This can be attributed to the CO_2 loading factor which is independent of liquid flow rate. As the absorbent velocity increases, the thickness of the mass boundary layer in the tube side decreases and improves the gas diffusion due to lower absorbent resistance. If the change in gas flow rate is considered to be negligible, the percentage of CO_2 removal can be defined as follows:

$$\%CO_2\ removal = 100\frac{(Q \times C)_{inlet} - (Q \times C)_{outlet}}{(Q \times C)_{inlet}} \quad (21)$$

where Q and C denote the gas volumetric flow rate (m³/s) and mole concentration (mol/m³), respectively. The concentration of CO_2 at the outlet of the shell side is calculated as follows:

$$C_{outlet} = \frac{\int C(r)dr}{\int dr} \quad (22)$$

and the mass transfer rate of CO_2 is expressed by the following equation:

$$J_{CO_2} = \frac{(Q \times C)_{inlet} - (Q \times C)_{outlet} \times 273.15 \times 1000}{22.4 \times T_g \times S} \quad (23)$$

where T_g (K) is the gas temperature and S (m²) is the total membrane area.

6 Conclusions

The modelling of CO_2 absorption by different amine solutions in hollow fibre membrane was studied. A comprehensive mathematical model was presented to determine the CO_2 concentration at the product stream under various operating conditions. The model was developed based upon continuity equations including diffusion and convection in shell and tube sides, and axial and radial diffusions through the membrane. COMSOL software was used to numerically solve a system of non-linear partial differential equations using the finite element method. The result of the suggested model was compared with experimental data obtained from the literature and a good agreement was observed. An increase in gas flow rate decreased the CO_2 mass transfer rate due to reduction of residence time and increase in liquid flow rate resulted in better removal efficiency due to the change in mass transfer

coefficient and the thickness of the absorbent boundary layer. Moreover, the flux of CO_2 could be improved by increasing absorbent concentration in the tube side due to availability of absorbent reactants at the gas-liquid interface. From three types of amine solution, MEA showed better performance for CO_2 removal as compared to the DEA and MDEA solutions. The results of modelling highlighted the importance and credibility of this model in order to determine more accurate CO_2 concentration using diverse types of absorbent in the HFMCs. The model developed has also more capabilities to be run with other type of absorbents for the membrane separation system in terms of absorbent selection.

Nomenclature

A	membrane surface area (m^2)
C	concentration (mol/m^3)
D	diffusivity coefficient (m^2/s)
J	molar flux (mol/m^{2}s)
H	Henry's constant
P	pressure (bars)
Q	flow rate (m^3/s)
R	reaction rate (mol/m^{3}s)
r_1	inner tube radius (mm)
r_2	outer tube radius (mm)
r_3	inner shell radius (mm)
T_g	gas temperature ($^\circ$C)
U	velocity (m/s)

Greek symbols

φ	module volume fraction
η	CO_2 removal efficiency

Abbreviations

HFMC	hollow fibre membrane contactor
DEA	Diethanolamine
MEA	Monoethanolamine
MDEA	n-methyldiethanolamine

References

1. Al-Marzouqi, M., El-Naas, M., Marzouk, S., Abdullatif, N., 2008. Modeling of chemical absorption of CO_2 in membrane contactors. Separation and Purification Technology 62(3), 499–506.
2. Albarracin Zaidiza, D., Billaud, J., Belaissaoui, B., Rode, S., Roizard, D., Favre, E., 2014. Modeling of CO_2 post-combustion capture using membrane contactors, comparison between one- and two-dimensional approaches. Journal of Membrane Science 455(0), 64–74.
3. Aroonwilas, A., Veawab, A., 2004. Characterization and comparison of the CO_2 absorption performance into single and blended alkanolamines in a packed column. Industrial & Engineering Chemistry Research 43(9), 2228–2237.
4. Baker, R., 2012. Membrane Technology and Applications. UK: John Wiley & Sons.
5. Bird, R.B., Stewart, W.E., Lightfoot, E.N., 2007. Transport Phenomena. US: John Wiley & Sons.
6. Casper, J.K., 2010. Greenhouse Gases: Worldwide Impacts. US: Infobase Publishing.
7. Chang, D., Min, J., Oh, S., Moon, K., 1998. Effect of pressure drop on performance of hollow-fiber membrane module for gas permeation. Korean Journal of Chemical Engineering 15(4), 396–403.
8. Faiz, R., Al-Marzouqi, M., 2009. Mathematical modeling for the simultaneous absorption of CO_2 and H_2S using MEA in hollow fiber membrane contactors. Journal of Membrane Science 342(1), 269–278.
9. Gilassi, S., Rahmanian, N., 2014. Mathematical modeling and numerical simulation of CO2/CH4 separation in a polymeric membrane. Applied Mathematical Modelling: pp. In Process.
10. Gilassi, S., Rahmanian, N., Year. An experimental investigation on permeability and selectivity of PTFE membrane: A mixture of methane and carbon dioxide. in *International conference on membrane science and technology (MST)* 2013. Malaysia, Kuala Lumpur: University Technology of Malaysia.
11. Halmann, M.M., Steinberg, M., 1998. Greenhouse Gas Carbon Dioxide Mitigation: Science and Technology. CRC press.
12. Happel, J., 1959. Viscous flow relative to arrays of cylinders. AIChE Journal 5(2), 174–177.
13. Hedayat, M., Soltanieh, M., Mousavi, S.A., 2011. Simultaneous separation of H_2S and CO_2 from natural gas by hollow fiber membrane contactor using mixture of alkanolamines. Journal of Membrane Science 377(1–2), 191–197.
14. Kothandaraman, A., Nord, L., Bolland, O., Herzog, H J., McRae, G.J., 2009. Comparison of solvents for post-combustion capture of CO_2 by chemical absorption. Energy Procedia 1(1), 1373–1380.
15. Li, J.L., Chen, B.H., 2005. Review of CO_2 absorption using chemical solvents in hollow fiber membrane contactors. Separation and Purification Technology 41(2), 109–122.
16. Mansourizadeh, A., Ismail, A.F., 2007. Hollow fiber gas-liquid membrane contactors for acid gas capture. 147–182.
17. Mills, A.F., 2001. Mass Transfer. Vol. 2. US: Prentice Hall.
18. Moulijn, J.A., Makkee, M., Van Diepen, A.E., 2013. Chemical Process Technology, 2nd ed., UK: John Wiley & Sons.
19. Nield, D., 2009. The Beavers–Joseph boundary condition and related matters: a historical and critical note. Transport in Porous Media 78(3), 537–540.
20. Paul, S., Ghoshal, A.K., Mandal, B., 2008. Theoretical studies on separation of CO_2 by single and blended aqueous alkanolamine solvents in flat sheet membrane contactor (FSMC). Chemical Engineering Journal 144(3), 352–360.
21. Rangwala, H.A., 1996. Absorption of carbon dioxide into aqueous solutions using hollow fiber membrane contactors. Journal of Membrane Science 112(2), 229–240.
22. Razavi, S.M.R., Razavi, S.M.J., Miri, T., Shirazian, S., 2013. CFD simulation of CO_2 capture from gas mixtures in nanoporous membranes by solution of 2-amino-2-methyl-1-propanol and piperazine. International Journal of Greenhouse Gas Control 15(0), 142–149.
23. Saidi, M., Heidarinejad, S., Rahimpour, H.R., Talaghat, M.R., Rahimpour, M.R., 2014. Mathematical modeling of carbon

dioxide removal using amine-promoted hot potassium carbonate in a hollow fiber membrane contactor. Journal of Natural Gas Science and Engineering 18, 274–285.

24. Sakwattanapong, R., Aroonwilas, A., Veawab, A., 2009. Reaction rate of CO_2 in aqueous MEA-AMP solution: experiment and modeling. Energy Procedia 1(1), 217–224.

25. Veawab, A., Aroonwilas, A., Tontiwachwuthikul, P., 2002. CO_2 Absorption Performance of Aqueous alkanolamines in Packed Columns. Fuel Chemistry Division Preprints 47(1), 49–50.

26. Versteeg, G.F., Van Swaalj, W., 1988. Solubility and diffusivity of acid gases (carbon dioxide, nitrous oxide) in aqueous alkanolamine solutions. Journal of Chemical and Engineering Data 33(1), 29–34.

27. Yan, S.P., Fang, M.X., Zhang, W.F., Wang, S.Y., Xu, Z.K., Luo, Z.Y., Cen, K.F., 2007. Experimental study on the separation of CO_2 from flue gas using hollow fiber membrane contactors without wetting. Fuel Processing Technology 88(5), 501–511.

28. Yang, J., Yu, X., Yan, J., Tu, S.T., Dahlquist, E., 2012. Effects of SO_2 on CO_2 capture using a hollow fiber membrane contactor. Applied Energy 112, 755–764.

29. Zhang, Y., Wang, R., 2013. Gas–liquid membrane contactors for acid gas removal: recent advances and future challenges. Current Opinion in Chemical Engineering, 255–262.

30. Zhang, H.Y., Wang, R., Liang, D.T., Wang, R. Liang, D T., Tay, J H. 2006. Modeling and experimental study of CO2 absorption in a hollow fiber membrane contactor. Journal of Membrane Science 279(1), 301–310.